Design and Control of a Force Reflecting Arm Exoskeleton for Virtual Reality Applications

Dimitar Chakarov, Ivanka Veneva, Mihail Tsveov and Dimitar Trifonov
Institute of Mechanics, BAS, Acad. G. Bonchev str. Block 4, Sofia, Bulgaria

Keywords: Exoskeleton Arm, Design, Haptic Device, Impedance Control, Pneumatic Muscle, Joint Torque, Antagonistic Interaction, Virtual Gymnastics.

Abstract: In this paper, the design of an exoskeleton for the upper limb is presented, aimed primarily at training and rehabilitation in virtual environments. A mechanical model of the exoskeleton arm as haptic device is built up and impedance control scheme is selected as the most suitable for force reflection at the arm. The design of a grounded exoskeleton prototype is revealed in the paper. A driving system based on braided pneumatic muscle is selected to ensure natural security in the interaction. Antagonistic drive system for each joint is shown, using pulley and Bowden cable transmissions. An approach is presented for the joint moments control by antagonistic interaction of bundles with different numbers of pneumatic muscles. Control scheme of joint torque by antagonistic interaction is given, too. Computer simulations are performed to provide power reflection by virtual reality (VR), according to scenario of virtual gymnastics.

1 INTRODUCTION

Exoskeleton is outside wearable robot with joints and limbs corresponding to those in the human body. Active exoskeletons transmit their driving mechanisms human joints moments. Exoskeletons are used in four main functions in accordance with their control algorithms (Perry, 2007): a) Rehabilitation - related closely to the body, they perform tasks of physical therapy in active or passive operation; b) Haptic device - people physically interact with virtual objects, as the forces of interaction apply to humans through the exoskeletons actuators; c) Master device - at control type "master-slave", the forces of interaction apply to exoskeleton - "master"by the robot-"slave"; d) Assisted human device - amplifier of the human body, the operator feels lighter loads, adopted by exoskeleton.

With the increase in recent years of applications, related to interaction in virtual environments increases the importance of the second function: using exoskeleton as Haptic device. Haptic interfaces allow humans to perceive and transmit forces and movement of real and virtual entities and actually to be "immersed" in virtual reality. It is possible to give people the illusion, that they have another body in immersion in virtual reality. When you move you see the virtual body to move in the same way (Slater, 2014), through motion capture in real time. This function for using exoskeletons is combined effectively with their other application - as a device for rehabilitation, using virtual scenarios.

In literature are presented many exoskeletons possessing very different mechanical structure and drive, with or without force feedback effect. The first modern exoskeleton of human upper limb was designed by PERCRO to feel and response in contact and collision with real and virtual entities (Bergamasco, 1994). The authors of PERCRO developed researches with designing other exoskeleton of human upper limb for Haptic interaction with virtual environments L-Exos (Frisoli, 2009).

Exoskeleton is known with pneumatic actuators, developed by (Lee, 1998). Their device is with 9 degrees of freedom and allows full playback of human hand workspace of exoskeleton. Alternative exoskeleton is developed by (Jeong, 2001), which is designed to overcome the limited bearing capacity of previous projects, using parallel mechanisms and pneumatic drives. Other examples of exoskeletons, targeted primarily for rehabilitation are ARMIN of the University of Zurich (Nef, 2007) and LDCs at the University of Salford, which uses pneumatic actuators (Tsagarakis, 2003). Comfortable to wear

Chakarov, D., Veneva, I., Tsveov, M. and Trifonov, D.
Design and Control of a Force Reflecting Arm Exoskeleton for Virtual Reality Applications.
DOI: 10.5220/0006427403350342
In *Proceedings of the 14th International Conference on Informatics in Control, Automation and Robotics (ICINCO 2017) - Volume 2*, pages 335-342
ISBN: Not Available

hand of Salford overcomes some of the problems and limitations of previous designs. This soft hand-exoskeleton is used for physiotherapy and for training.

These devices have to meet the safety requirements except the traditional requirements for performance. It is important to develop exoskeletons possessing naturally low impedance in order to achieve natural safety in the mutual interaction "man-robot".

One of the most common approaches to implement natural compliance is the usage of pneumatic artificial muscles (Daerden, 2002), (Tsagarakis, 2003), (Caldwell, 2007). The pneumatic muscles are actuators with a high power/weight ratio and can be directly coupled to the joint, without a heavy and a complex gearing mechanism. The force-deflection characteristic of these muscles, being strongly non-linear, they can be used to achieve compliance adjustment by means of an antagonistic setup. The drawbacks of the pneumatic muscles are: slow response to the input control, the presence of hysteresis, making precise position control difficult to realize and bringing the necessity of pressurised air.

Although various solutions are developed in order to be achieved simultaneous safety and performance within the human connected devices, there are still significant barriers that should be overcome (such as structure, drive and sense) to be able to provide natural, safe and comfortable physical interaction on the one hand and performance on the other. The objective of this work is to introduce the design of an active arm exoskeleton, ensuring natural, safe and comfortable physical interaction with human and to display force-related sensory information from a virtual environment to the user. The exoskeleton is designed primarily for training and rehabilitation in virtual environments.

2 MODELING AND CONTROL OF EXOSKELETON ARM

The device, which can be seen to function as a powered exoskeleton, is build-up of a branched serial structure, kinematics similar to the structure of the human body as it is shown in Figure 1.

The kinematics structure consists of four movable bodies 1, 2, 3, 4 and four rotational joints (Figure 1). The first two rotational joints J1, J2 are incident and mutually orthogonal in order to emulate the kinematics of a universal joint with the same centre of rotation as the human shoulder. The third and the fourth joints J3 , J4 are selected to be two rotational joints incident and mutually orthogonal in order to emulate the kinematics of a universal joint with the same centre of rotation as the human elbow flexion and human shoulder rotation. Moreover, the third joint was assumed to be coincident with the elbow joint as it is shown in Figure 1. The effective movements of so selected four joints simulate the movements of human arm in the shoulder and elbow. The exoskeleton upper limb structure has h = 4 degrees of mobility. This structure is chosen in order to construct an arm exoskeleton consisting of two equal type actuated universal joints.

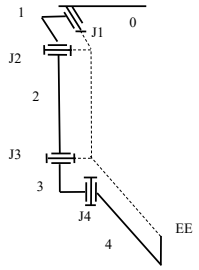

Figure 1: Structure scheme of exoskeleton arm.

Mechanical model of the upper limb exoskeleton is build up, according to the kinematics scheme shown in Figure 1. Generalized parameters are accepted to be the parameters of relative movements in the joints of exoskeleton represented by the (h x 1) vector $\boldsymbol{q}$. End-effector (EE) of exoskeleton arm moves in the ν - dimensional operation space. Assuming that the operator hand is connected at a point to the exoskeleton end effector, further we will consider exoskeleton operation space as 3 - dimensional. The coordinates of the exoskeleton end-effector are presented by (3 x 1) vector X. The relation between the generalized parameters q and the coordinates of the end-effector X is set by the direct kinematic problem. Regarding velocities, we formulate that problem by means of equality:

$$X = Jq \tag{1}$$

Above J is the (3 x 4) matrix of Jacoby.

To make the operator feel the simulated dynamics, impedance control is selected as the most suitable for force refection between the user and the virtual environment. The impedance model in Cartesian space is given by the following equation of simplified dynamics

$$Z\Delta X = -F \tag{2}$$

Above

$$\Delta X = [X; X; X - X_0]^T \quad (3)$$

is vector of end effector motion parameters, and

$$Z = [M; B; K] \quad (4)$$

is the mechanical impedance of the system in Cartesian space including the matrix of inertia, damping and stiffness *M, B*, and *K*.

An open-loop impedance controller with model-feedforward is selected (Carignan, 2000). This type of force control is called open-loop because there is no force feedback from the device to the controller to regulate the force output of the exoskeleton end effector as it is illustrated by the control block diagram in Figure 2. The goal of the model feedforward, is to cancel out the corresponding terms in the dynamics of the device. In control block diagram of Figure 2 the feedforward terms for the device stiffness and gravity are included. This scheme allows the use of so called strategy "patient-in-charge" when the patient lead the robot with a low impedance K_d and resistive forces are generated for deviations from the target in the virtual scene.

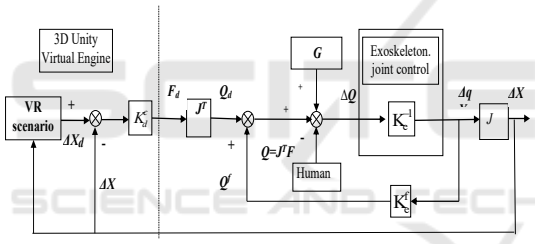

Figure 2: Block scheme of open-loop impedance controller with feedforward stiffness compensation.

According to this diagram, the controller takes the difference between the desired position deflection $\Delta X_d = X_d - Xo$, and the actual position defection of the haptic interface, $\Delta X \equiv X - Xo$. Since the positions on this linearized block diagram are represented by deviations from some nominal position *Xo*, the Cartesian position of the virtual interface and the joint position of the exoskeleton Δq are related through the Jacobian *J*. In this diagram, the exoskeleton natural stiffness is represented by joint-space stiffness K_e which is the relationship between the joint torque inputs and the differential angular output. The following relationships can be obtained from the block diagram

$$\Delta Q = Q_d + Q^f + G - Q \quad (5)$$

$$\Delta X = JK_e^{-1}[Q_d + Q^f + G - Q] \quad (6)$$

Above

$$Q_d = J^T F_d = J^T K_d^c [\Delta X_d - \Delta X] \quad (7)$$

represents desired force command in joint space. Similarly, in joint space the forces that the human exerts on the exoskeleton end effector are generated as:

$$Q = J^T F \quad (8)$$

Note, that *Q* represents a physical, not control input to the device. The term Q^f in (5) represents force command in joint space as a result of model feedforward compensation. It is calculated in accordance with modelled exoskeleton stiffness in joint space K_e^f according to equation

$$Q^f = K_e^f \Delta q = K_e^f J^{-1} \Delta X \quad (9)$$

The (h x 1) vector of (5):

$$G = [G_1, ..., G_h]^T \quad (10)$$

is the vector of gravity torques, generated at the exoskeleton joints. Its components:

$$G_j = \sum_{i=1}^{n} m_i g_o^T \frac{\partial \rho_i}{\partial q_j}, \; j = 1, \ldots, h \quad (11)$$

are determined by the mass of links m_i , i=1…n, the gravity acceleration vector in the base frame $g_0=[g_x, g_y, g_z]^T$ and the position vector of the i-th link centre of mass in the base frame $\rho^i = [\rho^x, \rho^y, \rho^z]^T$. After substituting equation (7), (8) (9) and (10) into (6) and setting $\Delta X_d = 0$, without loss of generality yields:

$$[K_e^c + K_d^c - K_e^{cf}]\Delta X = J^{-T} G - F \quad (12)$$

Above $K_e^c = J^{-T} K_e J^{-1}$ represents the natural stiffness of the exoskeleton in Cartesian space and $K_e^{cf} = J^{-T} K_e^f J^{-1}$ represents the stiffness model of the exoskeleton in Cartesian space. The influence of the member $[K_d^c - K_e^{cf}]$, that represents the active exoskeleton stiffness decreases, if the natural stiffness of the exoskeleton K_e^c is close to the desired level $K_e^c \Rightarrow K_d^c$. The aim is to develop an exoskeletons possessing naturally low impedance suitable for interaction with virtual objects where the value of the desired environment stiffness is low.

3 MECHANICAL DESIGN AND ACTUATION SYSTEM OF EXOSKELETON ARM

The mechanical structure of exoskeleton system includes two arms, that are grounded, as each arm is built up, according to structural diagram if Figure 1. Each arm has four active degrees of freedom, corresponding to the natural motion of the human arm from the shoulder to the elbow. Structure in Figure 1 is chosen in order to develop a powered exoskeleton arm, in which two equal type universal joints with 2 DoF are used and so, unlike other solutions, circular guide and three axes joints are avoided.

Each universal joint placed in the shoulder and in the elbow consists of a cross shaft and pair of rotational joint oriented at 90 ° to each other. The cross shaft is formed as an angle, in which the human hand is situated, as the axes of rotation intersect at a point, coinciding with the point of rotation of the human natural joint.

The basic parts of the exoskeleton arm structure are made of aluminium. The arm is constructed for use by a typical adult. All arm units are designed that allow quick and easy adjustment of length, so making it easy to accommodate a range of users. Plastic shells are placed over the units with bands for attachment to human limb. This design suggests a comfortable, light and low cost mechanical structure. In Figure 3, the structure of the right arm exoskeleton is shown, as a) is a computer simulation, and b) a picture of arm prototype. Exoskeleton left hand is designed as a mirror image of the right hand and is mounted on the common fixed base.

a) b)

a) computer simulation, b) picture of arm prototype.

Figure 3: Structure of the right exoskeleton hand:

Masses of the exoskeleton arm units are defined using CAD program. The masses of four basic units (Figure 1) are as follows m_1=0.437 kg, m_2=0.594 kg, m_3=0.364kg, m_4=0.434kg. Lengths of exoskeleton arm and forearm in the initial setup are as follows 0.286 m and 0.370 m respectively. The exoskeleton is designed so, that it covers the requirements of "Activities of daily living" (ADLs) as they have been assessed in (Perry 2007). The ADLs range of motions (ROM) and exoskeleton joint ranges of motions are shown in Table 1.

Actuation system of exoskeleton arm should have the following advantages: excellent power/weight ratio with inherent safety, natural compliance, low cost. To achieve these advantages self-made braided pneumatic muscle actuators (PMA) are used. PMA consists of two layers: an inner one, representing rubber liner and outer one, representing braided nylon. Endcaps are allocated at both ends, to which are clamped by clips the two layers. In one endcap is located a pipeline for supplying the pressurized air. Muscles possess a maximum diameter D_0 = 0.016 m and nominal length L_n =0.390 m. Thus created PMA are used not only singly, also in a sheaf of several pneumatic muscle, as shown in Figure 4.

Muscles from the bundle are fed in parallel with air at a maximum pressure 600 kPa (6 bar). Supply pipeline is connected with two parallel arranged valves of the type on / off, one of which serves to supply the maximum pressure and the other for discharge to the atmosphere. Pressure sensors are connected to the supply pipeline at every muscle bundle. All the muscles of the bundle are connected mechanically in one and at the other end, where they attach themselves.

Figure 4: Sheaf pneumatic muscle actuators.

Joint motion/torque on the exoskeleton arm is achieved by antagonistic actions through cables and pulleys, driven by the pneumatic actuators. Two sheafs PMA, a and b, work together in an antagonistic scheme, simulating a biceps-triceps system to provide the bidirectional motion/force, (Figure 5).

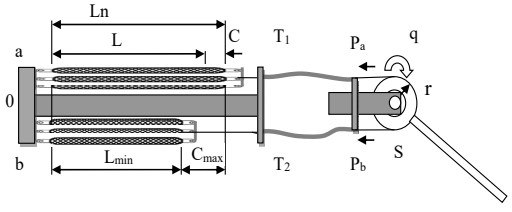

Figure 5: Antagonistic scheme for joint motion/torque.

Cable transmissions T_1 and T_2 are used for the coupling between the muscles and the pulley. The pulleys are fastened on the arm segments following joint shafts. All actuators are mounted on the exo-shell on the operator's back. High precision rotation sensors S are mounted in the joints.

According to the indications in Figure 5, muscle contraction is defined as:

$$C = L_n - L \tag{13}$$

Muscle contraction C is typically presented as a percentage of the nominal muscle length L_n determined by the outer braided layer $c=100\ C/L_n$.

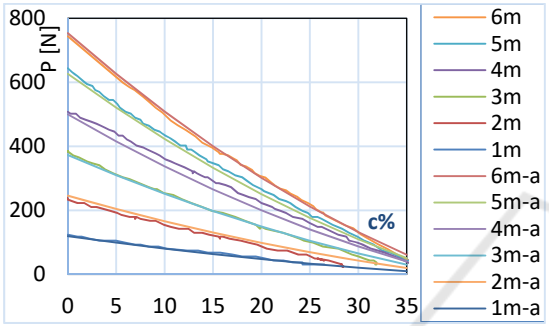

Figure 6: Graphs force / contraction of bundles of 1…6 muscles and their replicas at supply pressure of 400 kPa.

Experiments were conducted under static load of the used PAM, as the number of muscle in a bundle and the magnitude of the supply pressure has been altered. At set pressure, the contraction of muscles is measured by their nominal value L_n to a minimum value L_{min}.

Experimentally obtained force/ contraction diagrams (1m , … , 6m) for the used bundles consisting of 1 to 6 muscles at constant supply pressure of 400 kPa, are shown in Figure 6. At zero pressure the muscles show elastic properties determined of inner rubber liner. Pneumatic muscle behaves like a pressure dependent variable compliance spring. Graphs force/contraction of braided pneumatic muscle actuators typically represent quadratic functions. For replication of the used PAM as a nonlinear quadratic spring (Caldwell, 2007) can be used the following equation

$$P = K_p L(L - L_{min}) \tag{14}$$

where: P is the pooling force of the muscles, L and L_{min} are the muscle lengths according Figure 5, K_p is a pressure dependent coefficient. Taking into account (13) and equality for maximum contraction of muscle bundle $C_{max} = L_n - L_{min}$, equation (14) can be transformed

$$P = (k_o + tp)(L_n - C)(C_{max} - C) \tag{15}$$

where: p is the operating pressure, k_o and t are empiric derived coefficients that depend on the muscle number.

Approximated characteristics are composed for bundles from different number muscles m = 1,2,3,4,5 and 6 at a pressure p = 100, 200, 300 and 400 kPa. The maximum contraction of each muscle bundle is c_{max} = 40% Ln or C_{max}=0.156 m. In the process of approximation have been determined the following relations of the coefficients k_o and t in accordance with the number of bundle muscles m: $k_0 = -39 + 321$ m, $t = -0.21 + 4.41$ m.

Approximated characteristics of muscle bundles with 1, 2, ..., 6 muscles at a supply pressure of 400 kPa, are shown on Figure 6, (1m-a , … , 6m-a), where they are compared with experimentally obtained characteristics.

When the muscle bundles move the joint in an antagonistic scheme (Figure 5), the current contractions of each bundle in the joint C_a, C_b are determined by the joint end positions q_{max} , q_{min}.

To generate the maximum forces, muscles are attached so, as to operate with a minimum contraction, i.e., in the end joint position, one bundle has zero contraction and the contraction of the other is determined according to the equation

$$C_q = rq^* \tag{16}$$

where r is pulley radius and $q^* = (q_{max} - q_{min})$ is joint range of motion. Contraction (16) can be estimated as effective contraction of both muscles and to be presented as a percentage of the nominal muscle length L_n: $c_q = 100rq^*/L_n$. In each position of the joint, the equation (16) represents the sum of the preliminary contraction of the two muscle bundles.

In a current position q of the joint, the contractions of the two muscle bundles are

$$C_a = r(q^{max} - q) \tag{17}$$

$$C_b = C_q - C_a = r(q - q^{min}) \tag{18}$$

The forces P_a, P_b of joint muscle bundles can be calculated according to (15), (17) and (18). It is assumed, that one muscle sheaf is active in one direction, when the other is passive and vice versa at the sign change of the torque, establishing a maximum torque in the joint of antagonists muscle actuators. The muscle bundles with zero pressure always participate with a force in the joint antagonistic equilibrium, as they are elastic. Antagonistic balance in each joint is achieved by

generating desired torques in each joint, according to equality:

$$Q_i = (P_b - P_a)r \quad (19)$$

Since the bundle muscles with zero pressure (for example a) $p_a = 0$ generates elastic force P_a according to (15) end (17), draws (19), (15) and (18) allow to calculate the required pressure p_b of other muscles (for example b)

$$p_b = f(Q_i, q) \quad (20)$$

According to control block diagram on Figure 2, the joints torques Q_i are set from equality (5) as components of the vector representing force command in joint space

$$\Delta Q = [Q_1, ..., Q_i, .., Q_4]^T \quad (21)$$

The control scheme of the joint torque caused by the antagonistic interaction is shown in Figure 7. Pressures in the muscle bundles p_a and p_b are monitored by pressure sensors mounted to each muscle sheaf.

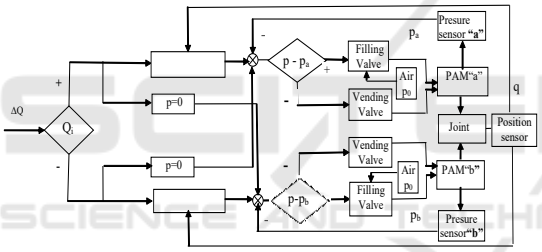

Figure 7: Control scheme of the joint torques.

A selection of bundles with different number of muscles in every joint is performed to ensure nominal torques in the joints and to provide joint moves q * (Chakarov, 2014). Selected bundles antagonists with number muscles m of the four arm joints are shown in Table 1. The table shows also achieved torques for each joint and muscles effective contractions.

For example, in Figure 8 is illustrated the change of the moment in the shoulder joint, under the influence of muscles antagonists a and b according to contraction in abduction/adduction: a) in abduction is active bundle b, which changes the pressure; b) in adduction is active bundle a and its pressure is changed. Shaded area of the chart shows the muscles work area, corresponding to the stroke of the joint. In this area, the achieved joint torque in according to (19) depends on contraction and is amended for shoulder abduction within the boundaries of 38.5 – 19.2 Nm, and for shoulder adduction within the boundaries of 4.7 - 13.9 Nm. Similarly, graphics are derived, amending moments in other joints. Table 1 shows the achieved torques for each joint.

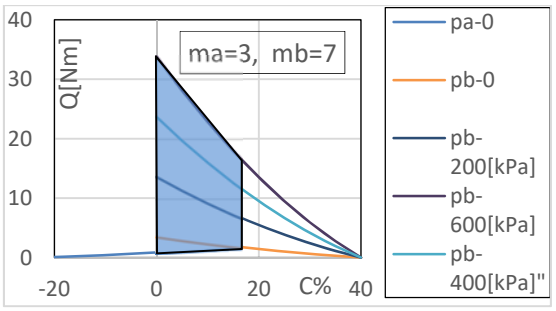

a)

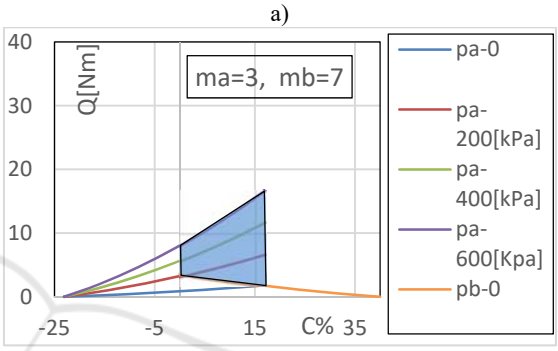

b)

Figure 8: Amendment of the torque in the shoulder joint under the influence of muscle bundles antagonists a and b: a) in abduction; b) in adduction.

4 COMPUTER EXPERIMENTS FOR ENSURING FORCE REFLECTION FROM VR

The exoskeleton is designed as a haptics device for applications in virtual reality. For example, one application is a virtual gymnastics. 3D Unity Virtual Engine is used for data transfer between exoskeleton and virtual entity (avatar) in virtual gymnasium. Optical tracker HMD Oculus Rift is used for visualization in the virtual system and to track the head position and orientation. Exoskeleton is designed to track position and orientation of human body and to provide force feedback to human arm. Figure 9 shows a scenario of virtual gymnastics - an exercise with fitness cable machine.

When the user set optical tracker attached to his head and "puts on the exoskeleton" as attaches the upper limbs to both arms of exoskeleton, he is "immersed" in the virtual scene gymnastics. Man gets the ability to transmit movement to the avatar and takes strength from it. One sees the virtual body to move like him, through motion capture in real time.

Table 1: ADLs and exoskeleton range of motions, effective muscle contractions, number of muscles and achieved torques.

		Bundles antagonists	ADLs range of motions [deg]	Exoskeleton range of motions [deg]	Effective muscle contractions c%	Number of the muscles in the bundle	Achieved torques [Nm]
Shoulder J1	Abduction	b	100	110	15.5	7	38.5 – 19.2
	Adduction	a			15.5	3	4.7 - 13.9
Shoulder J2	Flexion	b	110	120	16.9	6	32.9 – 16.2
	Extension	a			16.9	3	5.2 - 14.8
Elbow J3	Flexion	b	150	150	21.1	4	21.9 – 7.8
	Extension	a			21.1	2	2.0 – 9.8
Elbow J4	Int. rotation	b	135	135	19.0	4	21.7 – 7.2
	Lat. rotation	**a**			19.0	3	4.3 – 15.8

The controller in Figure 2 creates power commands in the joints of exoskeleton, that form the force action on the user's hands, equivalent to the power impact simulated in the virtual scene. In the scene of virtual gymnastics with cable machine, power influence is the tensile strength, which cable exerts on hand. The magnitude of this force is a constant, determined by the weight of the virtual weight stacks. For this scene, virtual machine generates a desired force command F_d in the controller in Figure 2, without taking into account the desired Cartesian stiffness K_d.

Figure 9: Scene of virtual gymnastics - an exercise with cable machine.

Simulations were conducted for assessing the projected exoskeleton ability to provide forceful impact on the operator, as the described scene of virtual gymnastics. Cable machine and the man's hand are simulated, as shown in the way in Figure 10. The figure shows the right arm in several positions, and the cable attached to the EE and slung over a roll in a fixed point T. Experiments were carried out in the following manner. A tensile force F is set, which virtual cable exerts on the avatar hand. This is the force, that exoskeleton must exercise over the hand of man. Exoskeleton arm performs a movement of maximum tension within the boundaries of joint ranges. Torques in the exoskeleton joints (5) were calculated by taking into account the desired moment $Q_d = J^T F_d$, as well as joint component of gravity compensation G. The desired force is assumed to be equal to the cable force with reverse sign $F_d = -F$. Gravitational component (10) were calculated after a preliminary masses and geometry assessment of the exoskeleton movable units.

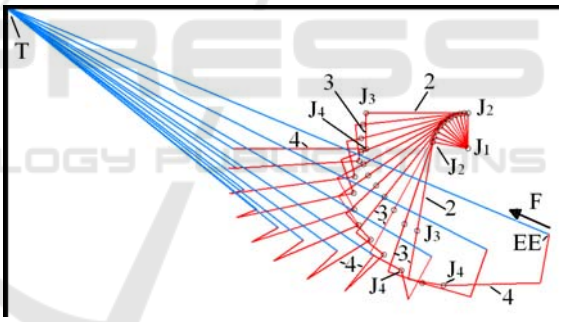

Figure 10: Simulation of the scene of virtual gymnastics with cable machine.

All joints are driven by antagonist bundles, consisting of different number muscles, performing effective muscle contractions, as shown in Table 1. Supply pressure for the active muscles changes on the range of 0 – 600 kPa, until the pressure of the passive ones is 0. The experiment shows that for values of the tensile force F = 0-50 N, desired torques in the joints of the exoskeleton are achievable within the limits of the attainable torques, shown in Table 1. In Figure 11 are shown the results of the shoulder joint at the movement "tension" with a force F = 50 N. It is shown the change of the joint components of the moments ΔQ, Q_d, G, as well as the achieved maximum moment in the joint Q_{max}, which is a result of the antagonist interaction of the bundles of muscles with maximum

and minimum pressure. On the X axis is given the contraction of active muscles bundle.

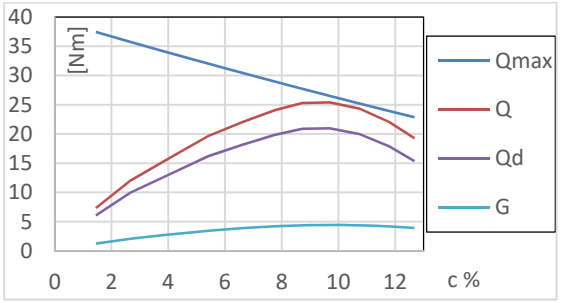

Figure 11: Amendment the joint components of ΔQ, Q_d, G, Q_{max}, in the shoulder joint at cable force of 50 N.

5 CONCLUSIONS

In this paper, the design of an active arm exoskeleton, aimed at human interaction with virtual environment is presented. In the work, a mechanical model of the exoskeleton arm, as haptic device is built up and impedance control scheme is selected for force refection at the arm. The design of a grounded exoskeleton prototype with low mass/inertial characteristics is revealed in the paper. To ensure natural security in the interaction, a driving system based on braided pneumatic muscle is selected. Antagonistic drive system for each joint is shown, using pulley and Bowden cable transmissions.

An approach for joint moments control by antagonistic interaction of bundles with different numbers of pneumatic muscles is presented. Computer experiments have been carried out to provide force reflection by VR, according to scenario of virtual gymnastics. The conducted simulations show the possibility of developed exoskeleton to provide impact strength of 50 N on the hand of the operator. Experiments with real exoskeleton prototype were conducted with volunteers, where they evaluate their feelings and their embodiment in a virtual scene. Additional measurements and evaluations of physical quantities are going to be performed.

ACKNOWLEDGEMENTS

This work was funded by the European Commission through FP7 Integrated Project VERE - No. FP7 - 257695 and by Bulgarian Science Found, Call: 2016, through Project AWERON – DN 07/9, to which the authors would like to express their deepest gratitude.

REFERENCES

Perry J., Rosen J, Burns S., 2007. Upper-limb powered exoskeleton design. *IEEE/ASME Transactions on Mechatronics*. Vol.12, No4, August 2007, pp. 408 – 417.

Slater M., Sanchez-Vives, M.V., 2014. Transcending the Self in Immersive Virtual Reality. *IEEE Computer 47 (7)*: 24-30 (2014), DOI: 10.1109/MC.2014.198.

Bergamasco M., B. Allotta, L. Bosio, L. Ferretti, G. Perrini, G. M. Prisco, F. Salsedo, And G. Sartini, 1994. An Arm Exoskeleton System for Teleoperation and Virtual Environment Applications, *IEEE Int'l Conf. Robot. Automat.*, vol. 2, 1449–1454.

Frisoli A., Fabio Salsedo, Massimo Bergamasco, Bruno Rossi And Maria C. Carboncini, 2009. A force-feedback exoskeleton for upper-limb rehabilitation in virtual reality, *Applied Bionics and Biomechanics,* Vol. 6, No. 2, June 2009, 115–126.

Lee,S., S. Park, M. Kim, And C.-W. Lee, 1998. Design of a Force Reflecting Master Arm and Master Hand using Pneumatic Actuators. *IEEE Conference on Robotics and Automation,* May 1998, 2574–2579.

Jeong Y., Y. Lee, K. Kim, Y. Hong, And J. Park, 2001. A 7 DOF Wearable Robotic Arm using Pneumatic Actuators," in *Proc. of the 32nd ISR International Symposium on Robotics*, April 2001, 388-393.

Nef T., M. Mihelji, and R. Riener, 2007. Armin: a robot for patient-cooperative arm therapy. *Medical & Biological Engineering & Computing*, 45 :887–900.

Tsagarakis N.G., Caldwell Dg., 2003. Development and control of a "soft-actuated" exoskeleton for use in physiotherapy and training. *Autonomous Robots.* 15(1):21–33.

Daerden Fr., D. Lefeber, 2002. Pneumatic Artificial Muscles: actuators for robotics and automation. *European Journal of Mechanical and Environmental Engineering,* 47(1), 1 - 11.

Caldwell D.G. et al., 2007. "Soft" exoskeletons for upper and lower body rehabilitation — design, control and testing. *International Journal of Humanoid Robotics* Vol. 4, No. 3, 549–573.

Carignan, C.R., K. R. Cleary, 2000. Closed- Loop Force Control for Haptic Simulation of Virtual Environments, *Haptics-e,* Vol. 1, No. 2, February 23, pp.1-14.

Chakarov, D., I. Veneva, M. Tsveov, T. Tiankov, D. Trifonov, 2014. New Exoskeleton Arm Concept Design and Actuation for Haptic Interaction with Virtual Objects, *Journal of Theoretical and Applied Mechanics*, Sofia, vol. 44, No 4, pp. 3-14, DOI: 10.2478/jtam-2014-00.